

CSIR–National Geophysical Research Institute, Hyderabad

Y. J. Bhaskar Rao*, Shakeel Ahmed, Vineet Gahalaut, Anil Kumar and M. Ravi Kumar

CSIR–National Geophysical Research Institute, Uppal Road, Hyderabad 500 007, India

The National Geophysical Research Institute, Hyderabad, under the aegis of the Council of Scientific and Industrial Research, New Delhi, continued its scientific pursuit in many important areas of basic and applied earth sciences research encompassing geophysics, geology, geochemistry, geochronology and geodesy during the year 2014. The Institute is credited with 167 research publications and has accomplished several national and international projects. We give in this article an overview of three select scientific achievements.

Keywords: Aquifer systems, Earth sciences research, mafic magmatism, seismic hazard.

3D imaging of aquifer systems: India's maiden heliborne geophysics experiment

CSIR–National Geophysical Research Institute, Hyderabad has successfully carried out state-of-the-art heliborne transient electromagnetic (HeliTEM) investigation and has obtained fascinating results on the aquifer systems and their spatial characteristics covering almost all types of geological formations present in the country. This study was in collaboration with the Central Groundwater Board (Ministry of Water Resources, River Development and Ganga Rejuvenation, New Delhi) and the Aarhus University, Denmark. The results, in general, helped in mapping the aquifers in three-dimension in desert, alluvium, hard rock and coastal tract and specifically for reconstructing the concealed subsurface spatial disposition of structures controlling the groundwater dynamics.

The HeliTEM method energizes the ground by means of sending a current pulse in the transmitter loop towed below the helicopter. The pulse induces eddy currents in the subsurface geological conductors that in turn produce secondary EM fields, which are recorded by a receiver loop, placed either at the centre or in close vicinity of the transmitter loop. This response is then analysed, processed and modelled to create depth images representing subsurface resistivity/conductivity distributions. Concurrent measurements of the magnetic field (HeliMAG) pro-

vide valuable information on the geological structures that control the occurrence of the groundwater. This system incorporates the unique feature of using dual (low and high) moments for the transmitter. While the initial measurements with low moment ($\sim 3400 \text{ A m}^2$) facilitate the measurement at very early times of about $9 \mu\text{s}$ to 1.7 ms , measurements at high moment ($155,000 \text{ A m}^2$) provide information in the late time range of about $84 \mu\text{s}$ to 8.9 ms . The early time measurements are particularly useful in deciphering the characteristics of shallow layers within a depth range $5\text{--}10 \text{ m}$. This information is critical for assessing the recharge potential of a region. The late time measurements provide reliable information about the deeper structures up to $\sim 300 \text{ m}$ illuminating signatures of potential aquifer systems. The unique advantage of such an investigation is that it does not suffer from the uncertainty of interpolation. For instance, in a typical scenario in the Ganga basin (Figure 1), the resolution of two distinct albeit closely disposed aquifers at different depths would not have been possible by conventional EM methods. Such resolution is paramount to decide the placement of a bore well because the shallower aquifer is plagued with arsenic contamination and water has to be carefully resourced from the deeper one that is arsenic-free.

In general, the resistivity depth sections are obtained using a laterally constrained inversion (LCI) procedure applied to data along various profiles and spatially constrained inversion (SCI) considering all the profiles in a particular region. The SCI inversion provides a 3D volume of the resistivity in the survey area enabling creation of horizontal slices or vertical sections along any arbitrarily chosen profile. For instance, Figure 2 shows geological maps, the total magnetic field from HeliMag and slices of mean resistivity map of 5 m thickness up to a depth of 150 m from HeliTEM, at a hard rock site in Tumakuru district, Karnataka. Notably, HeliMAG reveals a number of NW–SE, NE–SW and N–S faults, and dykes manifest as magnetic lineaments which were neither picked up in satellite imageries nor surface geological maps. The potential groundwater zones are inferred from magnetic lineaments. The magnetic lineaments in E–W and NE–SW directions are more suitable as revealed by the high-yielding well at Navule village (Tiptur Mandal). The dip of the fault plane could be inferred. The areas in

*For correspondence. (e-mail: director@ngri.res.in)

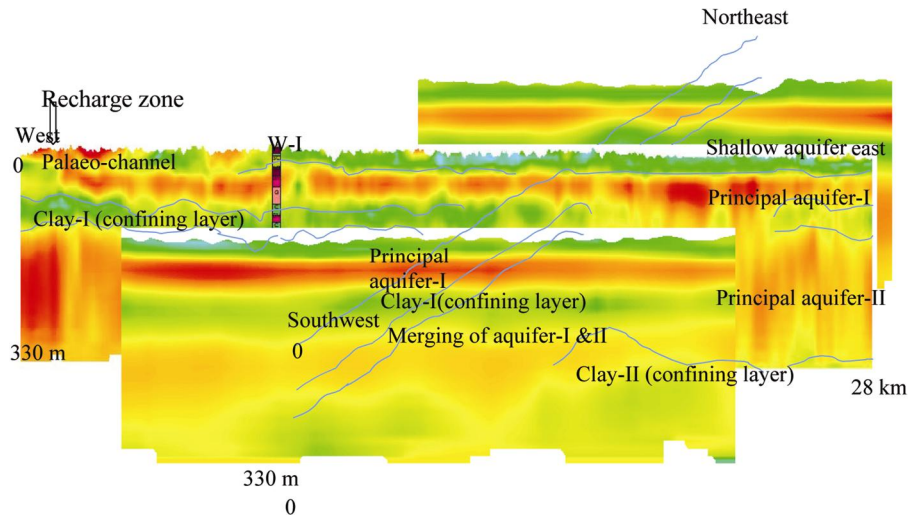


Figure 1. Continuous aquifer disposition in the alluvial tract of Ganga basin, Bihar.

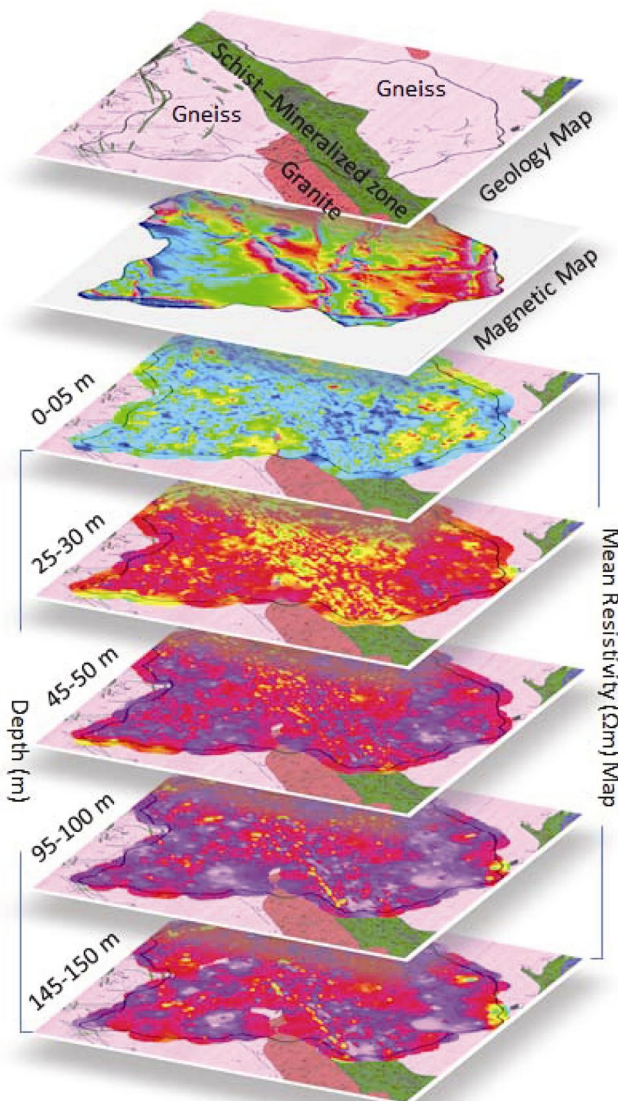


Figure 2. Maps of geology, total magnetic field and slices of mean resistivity in 5 m thick layers in a hard rock terrain, Karnataka.

proximity of the fault in downdip direction hold better groundwater potentiality. The contact between granite gneiss and schist is precisely delineated. The schist is found to be relatively more conductive than the gneisses and granites. In addition, potential base metal mineralized zones are apparent at different depth levels (Figure 2) demonstrating the applicability of the heliborne TEM data to mineral exploration apart from aquifer mapping.

The salient hydrogeological features of the six geologically distinct sites emerging from the pilot heliborne TEM experiment are summarized below:

- A clear delineation of clayey and sandy beds and their spatial distribution defining the multi-layered aquifer typical of the Gangetic Plains.
- Delineation of low resistivity zones in the quartzite below the overexploited aquifers indicating the possibility of new aquifers in a Precambrian sedimentary setting.
- Presence of comparatively freshwater zones underneath the saline water aquifers in the thick and dry sands in a desert.
- Clear demarcation of different lava flows, mapping the structural controls as well as highly porous zones at the contact between Deccan basalts and the underlying Gondwana strata.
- A complete and continuous mapping of weathered portions in the hard-rock (granite) terrain providing information on the recharge zones.
- The setting of multi-layered aquifer and different zones of salt-water intrusion in the coastal sedimentary formations.

The information afforded by the maiden heliborne experiment encourages upscaling to meet the country's groundwater requirement in diverse terrains.

Quantifying oblique motion and slip partitioning in the Himalayan arc: implications for seismic hazard

The Himalayan frontal arc accommodates about 2 cm/year of convergence of the India–Eurasia plate motion. This convergence is accommodated through stick and slip on the seismogenic detachment under the Outer and Lesser Himalaya. According to the oblique convergence model^{1–4}, the India–Eurasia convergence is arc normal in the Central Himalayan region but to the east and west of the region, it becomes oblique to the structural trend and frontal thrusts of the Himalaya. This obliquity results in partitioning in which the shear component is absorbed by pure shear on the generally east–west trending strike–slip faults in southern Tibet and predominantly arc-normal motion in the Himalayan frontal arc. GPS measurements have been useful in deciphering such complexities in tectonics and geodynamics, and also in constraining plate motion, convergence, slip partitioning and in assessing seismic hazard in the region. Such measurements in the Nepal region confirm that the entire motion of ~ 19 mm/year between southern Tibet and India⁵ is accommodated through thrust motion, with no oblique or shear motion in southern Tibet in the slip partitioning. To the west, in the Kashmir Himalaya, recent GPS measurements⁶ suggest that the oblique motion of 17 ± 2 mm/year between southern Tibet and the India plate is partitioned between dextral motion of 5 ± 2 mm/year on the Karakoram fault system and oblique motion of 13.6 ± 1 mm/year. The oblique motion in the frontal arc is also consistent with the *P*-axes of the earthquake focal mechanisms. Thus, the partitioning of the India–southern Tibet oblique motion is partial in the Kashmir Himalayan frontal arc. In this model, the Karakoram fault marks the northern limit of the NW Himalayan sliver. The Kaurik Chango rift, a north-south oriented seismically active cross-wedge trans-tensional fault, appears to divide the sliver in two parts causing varying translatory motion on the Karakoram fault on either side of the Kaurik Chango rift. Another important aspect of these measurements is their implication for seismic hazard. These measurements suggest a locking width of 175 km, against the locking width of ~ 100 km in the neighbouring Garhwal Kumaun and Nepal Himalaya. Elsewhere in the Himalaya, the earthquakes of Himalayan seismic belt⁷ and the 3.5 km topographic contour, coincide with the downdip edge of the locked zone⁸. However in the Kashmir Himalaya, they do not guide us to decide the width of the locked zone, as seismicity is almost absent and the 3.5 km topographic contour surrounds the Kashmir valley.

The Eastern Himalaya Syntaxis (EHS) in the far east along the arc is probably the most complex region and also another region where oblique motion is expected. Additionally, its limited accessibility has hampered seismological investigations leading to poor knowledge about

the geodynamic processes. GPS measurements of crustal deformation across the frontal EHS have been reported by Devachandra *et al.*⁹. In this region, the Indian plate obliquely underthrusts the Eurasian plate and the eastward extruding Tibetan plateau, due to India–Eurasia motion around the EHS. GPS measurements in the region suggest that the frontal EHS accommodates at least about 20 mm/year of oblique convergence comprising 17 ± 2 mm/year fault normal and 10 ± 3 mm/year fault parallel slip rate between the Indian and Eurasian plates. Presently, the 65 km wide detachment under the frontal EHS is locked leading to strain accumulation which may cause great or major earthquakes in future. Interestingly, the 3.5 km topographic contour also coincides with the downdip edge of the locked zone. These measurements and limited information about the great 1950 Assam earthquake (*M* 8.6) suggest that this earthquake probably occurred in the EHS.

Precise dating of mafic magmatism using TE-TIMS baddeleyite geochronology

The Earth's history has recorded numerous periods of accentuated mafic magmatism. Large igneous provinces (LIPs) that include continental flood basalts comprise magmas genetically unrelated to seafloor spreading and subduction. Several Proterozoic giant dyke swarms are mapped on a continental scale. These generally represent deeply eroded LIP sections. Precise age determination of such large dyke swarms not only enables establishing the incidence and extant of major magmatic events through time in a given region, but also provides geodynamic linkages to regional-scale uplift, continental rifting and break-up and climatic conditions. In conjunction with palaeomagnetic data, reliable age determination of dykes are important for Palaeo-continental reconstructions.

Precise U–Pb age determination of mafic magmatism ($\sim 0.1\%$ precision) has been possible mainly by the analysis of baddeleyite (ZrO_2) found as a common accessory mineral in the dyke and sill complexes. In contrast to zircon, baddeleyite generally contains sufficiently high concentrations of U (500 to several 1000 ppm) with concordant or nearly concordant (typically less than 1% discordance) U–Pb data even without any of the cumbersome pretreatment preparation required for zircon. This is because baddeleyite is much less susceptible to Pb loss than zircon and importantly, it rarely occurs as xenocrysts in these rocks. Due to such favourable physical and chemical properties, baddeleyite is considered to be an ideal mineral for U–Pb and Pb–Pb dating of mafic and ultramafic rocks.

Despite its potential as an ideal geochronometer for dating silica under-saturated igneous rocks (where zircons are extremely rare), baddeleyite age determinations are extremely sparse. This is partly because conventional U–Pb

dating by isotope dilution thermal ionization mass spectrometry (ID-TIMS) is restricted to only a few laboratories with the necessary ultra-clean environment, with Pb blanks of 1 pg or less required for precise determination of U and Pb elemental and isotopic compositions. Additionally, unlike the case of zircon and other U-rich minerals, high precision U–Pb age estimation of baddeleyite using high-resolution secondary ion mass spectrometry (SIMS) was not particularly successful until recently, owing to crystal orientation or twinning effects that bias the measured $^{206}\text{Pb}/^{238}\text{U}$ ratio, resulting in lower age precisions.

A novel method, thermal extraction-thermal ionization mass spectrometry, was recently developed at CSIR-NGRI¹⁰, wherein it was shown that Pb thermally extracted from baddeleyite into a silica-melt ionization activator produces strong ion beams that allow $^{207}\text{Pb}/^{206}\text{Pb}$ isotope ratios to be measured by a thermal ionization mass spectrometer to high precision ($\pm 10^{-4}$) with almost negligible contamination from common Pb. It was also demonstrated that the thermal extraction ^{207}Pb – ^{206}Pb ages are comparable with the conventional U–Pb ages in both accuracy and precision (less than 0.1%). This procedure does not need ultra-clean laboratory conditions, a prerequisite for conventional high-precision U–Pb geochronology, and hence can be easily practised in most TIMS isotope geochemistry laboratories. Using this method, the exact time of emplacement of several hitherto unknown LIPs was established in the Dharwar¹¹ and Singhbhum cratons¹², which are of paramount importance in establishing global correlations, enabling reconstruction and break-up of ancient cratonic nuclei and understanding large-scale geodynamic processes.

1. Seeber, L. and Pêcher, A., Strain partitioning along the Himalayan arc and the Nanga Parbat antiform. *Geology*, 1998, **26**, 791–794.
2. McCaffrey, R. and Nábelek, J., Role of oblique convergence in the active deformation of the Himalayas and southern Tibet plateau. *Geology*, 1998, **26**, 691–694.
3. Styron, R. H., Taylor, M. H. and Murphy, M. A., Oblique convergence, arc-parallel extension, and the role of strike-slip faulting in the High Himalaya. *Geosphere*, 2011, **7**, 582–596; <http://dx.doi.org/10.1130/GES00606.1>.
4. Murphy, M. A., Taylor, M. H., Gosse, J., Silver, C. R. P., Whipp, D. M. and Beaumont, C., Limit of strain partitioning in the Himalaya marked by large earthquakes in western Nepal. *Nature Geosci.*, 2013, **7**, 38–42; doi:10.1038/NGEO2017.
5. Ader, T., *et al.*, Convergence rate across the Nepal Himalaya and interseismic coupling on the Main Himalayan Thrust: implications for seismic hazard. *J. Geophys. Res.*, 2012, **117**, B04403; doi: 10.1029/2011JB009071.
6. Kundu, B., Yadav, R. K., Bali, B. S., Chowdhury, S. and Gahalaut, V. K., Oblique convergence and slip partitioning in the NW Himalaya: implications from GPS measurements. *Tectonics*, 2014, **33**, 10.1002/2014TC003633.
7. Cattin, R. and Avouac, J. P., Modeling mountain building and the seismic cycle in the Himalaya of Nepal. *J. Geophys. Res.*, 2000, **105**, 13389–13407.
8. Avouac, J.-P., Mountain building, erosion and the seismic cycle in the Nepal Himalaya. *Adv. Geophys.*, 2003, **46**, 1–80.
9. Devachandra, M., Kundu, B., Joshi, C., Arun Kumar and Gahalaut, V. K., First GPS results of crustal deformation across the frontal Eastern Himalayan Syntaxis and seismic hazard assessment. *Bull. Seismol. Soc. Am.*, 2014, **104**, 1518–1524.
10. Kumar, A., Nagaraju, E., Srinivasa Sarma, D. and Davis, D. W., Precise Pb baddeleyite geochronology by the thermal extraction–thermal ionization mass spectrometry method. *Chem. Geol.*, 2014, **372**, 72–79.
11. Kumar, A., Hamilton, M. A. and Halls, H. C., A paleoproterozoic giant radiating dyke swarm in the Dharwar Craton, southern India. *Geochem. Geophys. Geosyst.*, 2012, **13**(2), DOI:10.1029/2011GC003926; http://scholar.google.com/citations?view_op=view_citation&hl=en&user=OFjwXtEAAAAJ&sortBy=pubdate&citation_for_view=OFjwXtEAAAAJ:RtRctb2ISbAC.
12. Shankar, R., Vijaya Gopal, B. and Kumar, A., Precise Pb–Pb baddeleyite ages of 1765 Ma for a Singhbhum ‘newer dolerite’ dyke swarm. *Curr. Sci.*, 2014, **106**(9), 1306–1310.